Journal of Thermal Analysis and Calorimetry, Vol. 78 (2004) 349–361

TMDSC ANALYSIS OF SINGLE-SITE COPOLYMER BLENDS AFTER THERMAL FRACTIONATION

G. Amarasinghe and R. A. Shanks[*]

Department of Applied Chemistry, RMIT University, GPO Box 2476V, Melbourne, Victoria 3001, Australia

(Received February 16, 2004; in revised form April 22, 2004)

Abstract

Temperature-modulated differential scanning calorimetry (TMDSC) has been used to study the melting of a series of blends containing linear low-density polyethylene (LLDPE) and very low-density polyethylenes (VLDPE) with long chain branches. After the blends were subjected to different thermal histories including thermal fractionation by stepwise isothermal cooling, they were examined by TMDSC. TMDSC curves have been interpreted in terms of a combination of the reversing and non-reversing specific heats that result from reversible and irreversible events at the time and temperature, which they are detected, respectively. It was found that crystals formed at different crystallisation conditions had different internal order; hence they showed different amounts of reversing and non-reversing contributions. There is no exothermic activity seen in the non-reversing signal for the thermally fractionated polymers and their blends suggesting formation of crystals approaching equilibrium. In contrast, polymers and blends cooled at 10°C min^{-1} cooling rate showed large exothermic contributions corresponding to irreversible effects. In addition, a true reversible melting contribution is also detected for both fast-cooled and thermally-fractionated samples during the quasi-isothermal measurements.

Keywords: ethylene-octene copolymer, metallocene polyethylene blends, reversible melting, thermal fractionation, TMDSC

Introduction

Differential scanning calorimetry (DSC) has long been a valuable technique that is used to study melting and crystallisation behaviour and the morphology of polymers. However, the interpretation of a DSC scan is often ambiguous because it contains many non-equilibrium effects. Temperature modulated differential scanning calorimetry (TMDSC) has been established as an alternative technique to produce new and different quantitative information on thermal transition of polymers relative to conventional DSC [1–3], and its theory and operating principles are extensively described elsewhere [1–6]. TMDSC uses a periodical temperature modulation over a traditional linear heating or cooling ramp and is capable of giving accurate heat ca-

* Author for correspondence: E-mail: robert.shanks@rmit.edu.au

1388–6150/2004/ $ 20.00

Akadémiai Kiadó, Budapest
Kluwer Academic Publishers, Dordrecht

pacity measurements and separating underlying kinetic and thermodynamic phenomena with better resolution and sensitivity [7].

There are two main approaches to analyse the resulting modulated heat flow: reversing/non-reversing (NR) total heat flow or heat capacity approach described by Reading *et al*. [1, 2] and complex heat capacity approach by Schawe [3]. Despite the method used, three types of curves can normally be derived from the modulated DSC experiments: total heat flow or heat capacity curve (total C_p, same as conventional DSC curve), in-phase curve (reversing or storage) and out-of-phase curve (kinetic or loss) [8]. In addition, the non-reversing heat capacity curve (C_{pNR}) can be obtained by the difference between the total C_p and reversing heat capacity (C'_p). This curve is particularly useful for determining irreversible processes such as enthalpy relaxation, evaporation, cold crystallisation, chemical reactions, curing, decomposition and recrystallisation. The reversing curve represents the effects that are thermodynamically reversible at the time and temperature at which they are detected, whereas the out-of-phase curve is expected to show irreversible phenomena within the modulation conditions. The out-of-phase component is calculated by the phase angle shift between the calorimetric response and modulated program, which will significantly influenced by the heat transfer effects [6, 9, 10]. Therefore, the interpretation of the out-of-phase component is dubious and the results here are presented and discussed using the reversing and non-reversing curves.

Melting of a polymer provides complex situation, because a polymer structure can undergo various transformations, such as recrystallisation, crystal annealing and perfection during heating [11]. TMDSC has been used to analyse the crystallisation and melting of various polymers as thoroughly reviewed by Wunderlich [12], with polyethylenes studied most widely [12–31]. The current view is that the processes of crystallisation and melting of polyethylenes are mostly thermodynamically irreversible and a non-reversing (irreversible) character associated with recrystallisation, crystal annealing and perfection of the non-equilibrium crystals are observed under temperature modulation conditions [12, 15–30]. Nonetheless, the melting and crystallisation of well-crystallised low molar mass polyethylenes [20], poly(oxyethylene) [4, 31, 33] and *n*-paraffins [4, 29] are largely reversible and they become irreversible with increasing chain length and molar mass [23]. In addition, another process, so-called reversible melting was observed. It produces a reversible component in the reversing endotherm in the absence of other irreversible processes such as recrystallisation, crystal annealing and melting [19–23]. This can be detected under the quasi-isothermal (QI) mode, i.e., modulation about a constant temperature, which allows delaying measurements until the completion of other irreversible processes. This is expected to be aroused by molecular nucleation, in which some of the molecules that have melted recrystallise onto the existing crystals with negligible cooling. The six contributions, three reversible (thermodynamic heat capacity, heat capacity due to conformational motions, reversible melting) and three irreversible (crystal perfection, secondary crystallisation and primary crystallisation) to apparent heat capacity in melting and crystallisation regions were suggested by Wunderlich *et al*. [18].

Blends of polyethylenes produced from single-site catalyst technology are widely used in film industry. These polymers have more branches than conventional

linear-low density polyethylenes (LLDPE) and the branches are more evenly distributed along the polymer chain due to the single-site nature of the catalyst used in the polymerisation. We have prepared blends of single-site catalysed VLDPEs (very low density polyethylene) having long chain branching with Ziegler-Natta catalysed LLDPE. Their morphology and miscibility were investigated and reported in our previous publication [34]. The crystallisation and melting behaviour obtained by DSC after the DSC thermal fractionation (TF) technique, which separate molecules according to the branching densities suggest co-crystallisation and partial miscibility of blends having high VLDPE contents. The aim of this study is to employ TMDSC technique to understand the complex structures and melting behaviour of LLDPE-VLDPE blends. Thermal transitions and crystallinity of blends, after crystallising blends at different crystallisation conditions were investigated. Since TMDSC is capable of measuring the dynamic processes inside the sample during the temperature scanning, it is of interest to combine the various sample thermal histories with TMDSC melting analysis.

Experimental

The properties of polymers (Orica Ltd., Australia) used are shown in Table 1. The polyethylenes were chosen to have similar branch length and were octene copolymers. LLDPE was blended with VLDPE1 or VLDPE2 using an Axon single-screw extruder (Axon Australia Pty. Ltd., Australia) using a Gateway screw (L=12.5 mm, L/D=26) and the blends were mixed in various proportions 10, 20, 50 and 80% (by mass) and details of preparation of blends are reported in elsewhere [34]. The films of 1 mm thickness were prepared by pressing pellets in a hot press at 150°C for 5 min.

Thermal treatments and thermal analyses were performed in a Perkin Elmer Pyris1 DSC (Perkin Elmer Instruments, Norwalk, CT, USA). The DSC was operated at ambient temperature mode with a cold finger cooled to 1–5°C with ice/water and dry nitrogen gas with a flow rate of 20 mL min^{-1} was purged through

Table 1 Characteristics of polymers

Properties	LLDPE[a]	VLDPE1[b]	VLDPE2[b]
Comonomer	octene	octene	octene
Catalyst type[e]	ZN	S	S
MFI/°C min^{-1}	0.94	1.0	1.0
Density/g cm^{-3}	0.927	0.915	0.908
M_w/g mol^{-1}	133000	97800	96700
M_w/M_n	6.6	2.6	2.86
Comonomer content/mass%	2.7	7.5	9.5

[a][35], [b][36], [e]ZN=Ziegler–Natta catalyst, S=Constrained Geometry Single-site catalyst

the sample. The flat, single film samples of 2–4 mg were used to minimize the thermal lag [37]. Two different thermal treatment methods were followed: continuous cooling at a 10°C min^{-1} rate from the melt and stepwise crystallisation (thermal fractionation) at an average rate of 0.08°C min^{-1} from the melt [isothermal crystallisation for 50 min from 122–46°C in every 4°C; Detailed procedure is published in [32]. Before applying the particular thermal treatment, previous thermal memory of all the samples was removed by holding at 180°C for 5 min. The melting scans of treated samples were obtained by using the saw-tooth modulation and the modulation parameters were chosen so that the sample was always heated. The underlying heating rate of 2°C min^{-1} with temperature amplitude of 0.5°C and an oscillation period of 60 s (frequency=16.7 mHz) were used for modulated experiments. The scanned temperature range was from 30 to 150°C. A baseline was recorded with similar empty pans (30 μL) using the same method. The calorimeter was calibrated for temperature using cyclohexane, indium and zinc standards and the temperature calibration was regularly checked *vs.* the melting onset temperature of indium. The heat flow calibration was performed using indium. The heat flow data from the modulated scans were then used to calculate the total heat capacity (total C_p) and C_p'. The C_{pNR} curve was obtained by subtracting the C_p' curve from total C_p curve. QI mode experiments with oscillation frequency of 16.7 mHz, temperature amplitude of 0.5°C and zero underlying heating rate were carried out as described by Ishikiriyama and Wunderlich [33]. The crystallinity (X) was calculated from the enthalpy of total heat capacity curves [ΔH (total C_p)] taken from 35–135°C. The heat of fusion value for 100% crystalline polyethylene was taken as 293 J g^{-1} [38].

Results and discussion

TMDSC of continuously cooled samples

Figure 1a shows the total C_p melting curve of LLDPE, VLDPE2 and their blends obtained after continuous cooling at 10°C min^{-1}, while Figs 1b and c show the corresponding C_p' and C_{pNR} curves. The melting temperatures, heat of fusion and crystallinity values are given in Table 2. The melting can be seen in all three curves of pure LLDPE. The total C_p curve of LLDPE (bottom curve) showed a broad melting endotherm with multiple melting peaks (116.0, 119.5, 122.0°C) corresponding to melting of a wide range of crystallite distribution. LLDPE is prepared by solution/slurry polymerisation via Ziegler-Natta catalyst and it has an irregular branching distribution with a broad molecular mass distribution due to the multiple active sites of the catalyst. Therefore, the bimodal lamellar thickness distribution with double crystalline morphology, which is typical for all LLDPE's, is also observed for LLDPE. A transmission emission microscopy study performed by Hosoda *et al.* has revealed that LLDPE generally exhibits two different types of lamellae; thick, long and straight lamellae like those of high density polyethylene, and thin, short and curved lamellae that grow among the former ones [39]. In contrast, the total C_p curve of single-site catalysed

Table 2 TMDSC data of continuously cooled samples at 10°C min^{-1}

Polymer and blends	T_{m1}/°C	T_{m2}/°C	T_{m3}/°C	T_{m4}/°C	ΔH (total C_p)/J g^{-1}	ΔH (C_p')/J g^{-1}	ΔH (C_{pNR}/J g^{-1}	X/%
LLDPE	116.0	119.5	122.0		106.0	110.1	–4.1	36.5
VLPPE1	111.2				88.6	139.6	–51.0	30.5
VLDPE2	106.1				81.3	124.5	–43.2	28.0
10% VLDPE1	108.4	119.0		123.2	84.4	158.7	–74.3	29.1
20% VLDPE1	109.2	119.3	121.9	123.8	93.5	164.4	–70.9	32.2
50% VLDPE1	108.5	116.8	121.7	124.6	72.2	191.3	–119.1	24.9
80% VLDPE1	110.0	113.6	120.0	122.2	65.8	173.2	–107.4	22.9
10% VLDPE2	110.0	119.8	122.2	123.9	98.0	168.8	–70.8	33.8
20% VLDPE2	107.3	119.0		123.2	111.1	218.6	–107.5	38.3
50% VLDPE2	108.9	117.0	120.9	123.5	98.9	225.1	–126.2	34.1
80% VLDPE2	105.4		120.8	124.1	96.0	208.1	–112.1	33.1

[a]Peak melting temperatures of the total heat capacity curve

VLDPE2 (top curve) displayed a much narrower melting peak at 106.1°C due to the more evenly distributed branches along the polymer backbone.

The analogous melting behaviour was also observed in the corresponding C_p' curves of LLDPE and VLDPE2 (Fig. 1b, bottom and top curves, respectively), but displayed a much broader and larger single endothermic signal. Continuous melting during the heating scan was also observed for polymers starting from about 50°C by the gradual increase of the C_p' over the baseline. Interestingly, the corresponding C_{pNR} curves (Fig. 1c) illustrated that certain exothermic activity was involved before

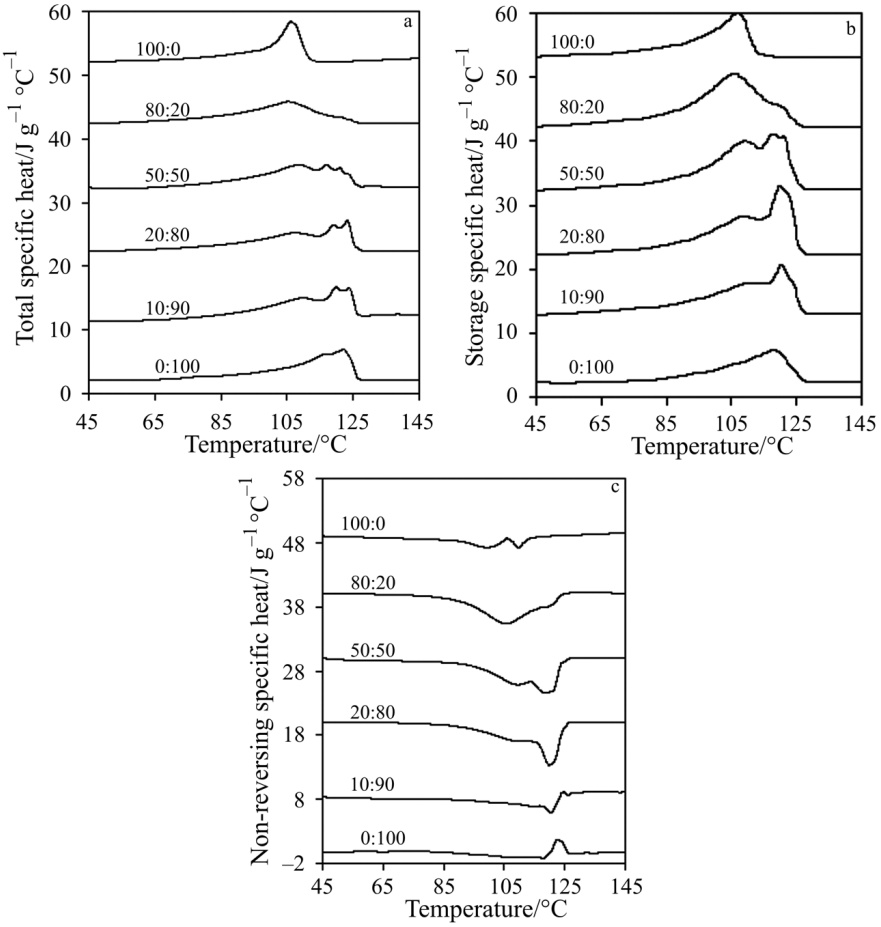

Fig. 1 Modulated specific heat curves of continuously cooled LLDPE, VLDPE2 and their blends at 10°C min^{-1}; a – total specific heat curves; b – reversing specific heat curves and c – non-reversing specific heat curves. Modulation parameters are f=16.7 mHz, T_a=0.5°C and β_0=2°C min^{-1}. An adapted scale is drawn by consecutively adding 10 units to each curve. First number of the ratio indicates the VLDPE2 amount

and during the melting of LLDPE and VLDPE2. The C_{pNR} curve of VLDPE2 characterises two separate exotherms at 100.0 and 109.9°C with a middle endotherm at 106.0°C where the main melting peak appeared (Fig. 1c, top curve), whereas, a broad exotherm from 75–118.0°C and an endotherm at 122.2°C were observed for LLDPE (Fig. 1c, bottom curve).

Similar results were also observed for the melting of blends, treated by continuous cooling at 10°C min^{-1}. All blends, except 90:10 LLDPE:VLDPE2 blend, showed only endothermic melting in the total C_p and C_p' curves and only exothermic peaks in the C_{pNR} curves. Conversely, the C_{pNR} curves of 90:10 LLDPE:VLDPE2 blend contained both endothermic and exothermic peaks, as in LLDPE. The exothermic only or both endothermic and exothermic behaviour of C_{pNR} curve has also been observed for other polymers such as poly(ethylene 2,6-napthalenedicarboxylate) (PEN) depending on the crystal stability [40, 41]. The presence of an exothermic NR contribution suggested that all copolymers and blends experienced significant recrystallisation and/or annealing throughout the heating process. Moreover, the data indicated that recrystallisation and/or annealing processes of LLDPE in the main melting region were not as dominant as in the case of VLDPE2. As it can be seen from Fig. 1c, polymers showed recrystallisation exotherm that started immediately after the partial melting of initial crystals at lower temperature. The exothermic peak prior to melting in the C_{pNR} curves indicated that recrystallisation and annealing of crystallites preceded on heating as a consequence of the metastable crystals formed by the cooling treatment at a rate of 10°C min^{-1}. Therefore, the process of melting, recrystallisation and remelting (mrr) occurs in these samples, and the reversing curve corresponds to the melting of primary crystals and remelting of secondary crystals. Nevertheless, the standard DSC curves (Fig. 7 in [32]) or total C_p curves did not indicate any recrystallisation during the scanning since it was cancelled by the broad endotherm.

The enthalpies of reversing and NR components are shown in Table 2. It is known that poorly crystallised polymers have relatively larger reversing melting contribution while perfect crystals show a little or none [22]. The reversing components of continuously cooled samples were large, suggesting that the most of metastable crystals were formed in these samples. Therefore, the presence of large reversing contribution along with exothermic NR contribution verifies the formation of thermally unstable crystals. The crystallinity values calculated based on the heats of fusion of total curves showed a gradual decrease in crystallinity upon addition of branched VLDPE2. As was previously seen in the standard DSC melting curves (Fig. 7 in [34]), the total C_p curves of LLDPE-VLDPE2 blends showed a broad distribution of melting with three or four peak temperatures. Nevertheless, the much better resolved peaks were seen in the total heat capacity curve perhaps due to the higher sensitivity of the modulated experiments. The C_p' curves shown in Fig. 1b displayed three melting peaks in most blends; a broad lower temperature peak, a sharper main melting peak with a shoulder on its higher temperature side.

Blends of LLDPE-VLDPE1 (not shown here) showed comparable melting behaviour. VLDPE1, which has slightly fewer branches than VLDPE2, exhibited the same behaviour, i.e., two separated exotherms at 103.8 and 113.7°C with a middle endothermic peak at 111.0°C where the main melting peak appeared (not shown

here). The total specific heat and C_p' curve of VLDPE1 detected a relatively sharp narrow peak at 111.2°C.

TMDSC of thermally fractionated samples

The thermal treatment here is the stepwise isothermal crystallisation, which is designed to fractionate polymers in a DSC, on the basis of the branching distribution [34, 42–44]. It involves the same principle of separation as temperature rising elution fractionation that fractionates copolymers based on crystallisability. Thermal fractionation, i.e., 50 min isothermal crystallisation steps in every 4°C from 122–46°C (average rate of 0.08°C min^{-1}), creates a series of discrete melting peaks as seen in Fig. 2. The crystals

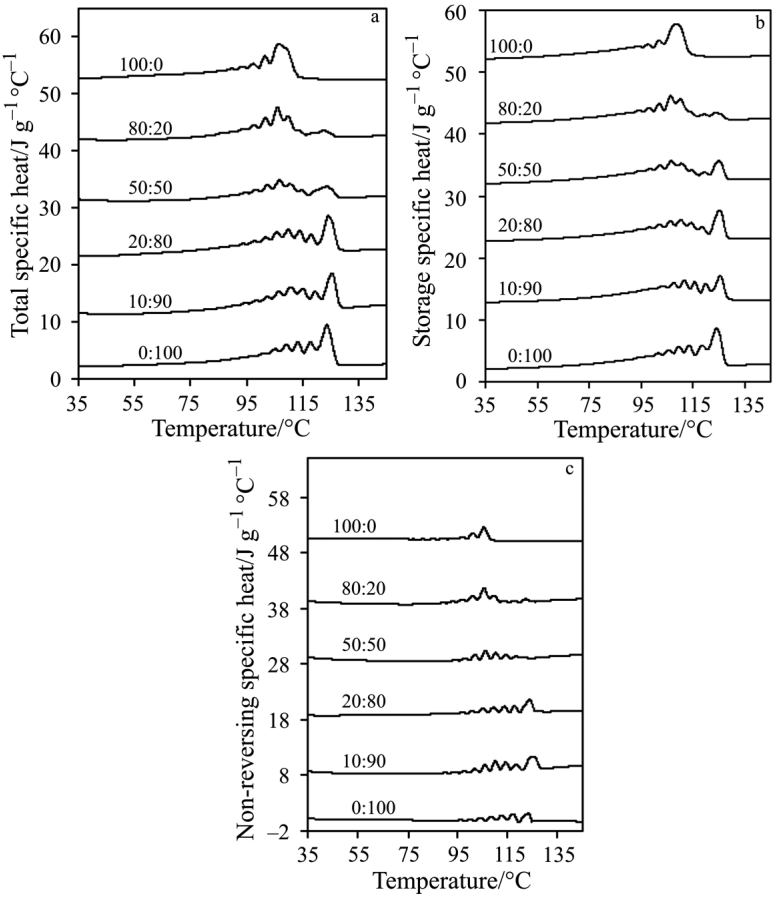

Fig. 2 Modulated specific heat curves of stepwise-cooled (thermally fractionated) LLDPE, VLDPE2 and their blends; a – total specific heat curves; b – reversing specific heat curves and c – non-reversing specific heat curves. Modulation parameters are f=16.7 mHz, T_a=0.5°C and β_0=2°C min^{-1}. An adapted scale is drawn by consecutively adding 10 units to each curve. First number of the ratio indicates the VLDPE2 amount

represented by each peak have been formed under isothermal conditions over a time of 50 min. At any particular isothermal temperature, polymer chains with similar branch densities are separated and crystallised together. During the crystallisation, the branch points and short branches are excluded from the crystal and the long ethylene segments will form chain-folded lamella crystals. Since the branches and branch points are excluded from the lamellae, the distance between branches determines the lamella thickness, which is then determined by the subsequent melting of each fraction [42–44].

Table 3 TMDSC data of stepwise-cooled (thermally fractionated) samples

Polymer and blends	ΔH (total C_p)/J g^{-1}	ΔH (C'_p)/J g^{-1}	ΔH (C_{pNR})/J g^{-1}	X/%
LLDPE	124.5	104.2	20.3	42.9
VLPPE1	115.5	101.4	14.1	39.8
VLDPE2	100.9	88.7	12.2	34.7
10% VLDPE1	119.9	106.9	13.0	41.3
20% VLDPE 1	113.2	97.8	15.4	39.0
50% VLDPE1	113.1	97.9	15.2	39.0
80% VLDPE1	114.7	111.8	2.9	39.5
10% VLDPE2	101.7	98.9	2.8	35.0
20% VLDPE2	116.7	100.9	15.8	40.2
50% VLDPE2	108.6	82.8	25.8	37.4
80% VLDPE2	107.3	103.1	4.0	37.0

Unlike in case of continuously cooled samples, all three curves of fractionated samples including C_{pNR} curves showed essentially endothermic contributions. The total C_p curves shown in Fig. 2a exhibited a series of melting endotherms that were similar to those of conventional DSC curves previously observed for the thermally fractionated copolymers (Fig. 6 in [34]). Since the crystallisation temperatures are predetermined, the melting peak temperatures are artificially created and are the same for identical fractions. The corresponding C'_p curves shown in Fig. 2b also exhibited a similar shape, but the maximum peak temperatures of some peaks were slightly changed by shifting of 0.5–2°C to a higher temperature than those of total C_p curves. Surprisingly, the C_{pNR} curves of pure polymers and blends (Fig. 2c) showed mainly endothermic peaks, suggesting the absence of recrystallisation and/or annealing of thermally fractionated crystals during melting. As discussed before, during the thermal fractionation, samples were crystallised at an extremely slow average cooling rate (0.08°C min^{-1}). Consequently, the crystals were expected to approach an equilibrium state and form highly ordered crystals, and these crystals were less likely to rearrange during heating. In fact, Liu *et al*. have shown by simultaneous X-ray scattering techniques that significant crystal perfection occurs during the thermal fractionation of polyethylenes [44]. Such endothermic only C_{pNR} contributions have been reported for well-crystallised PEN samples annealed at higher temperatures by

Kampert and Sauer [40]. The changes in specific heat curves of the LLDPE-VLDPE2 blends are indicative of a dilution effect whereby the two polymers have co-crystallised according to their branch distribution.

The reversing contributions given in Table 3 were also much less than those of the continuously cooled samples (Table 2) because of the melting of more stable crystals having highly ordered lamella formed under slow crystallisation conditions provided by the very slow stepwise cooling process. The higher ordering of crystals is further evident by crystallinity values of fractionated samples shown in Table 3, which shows much higher crystallinity values than those of continuously cooled blends. All these data support the fact that the crystals formed during the thermal fractionation are much more stable and closer to equilibrium than continuously cooled samples. A similar trend was also observed for the thermally fractionated LLDPE-VLDPE1 blends.

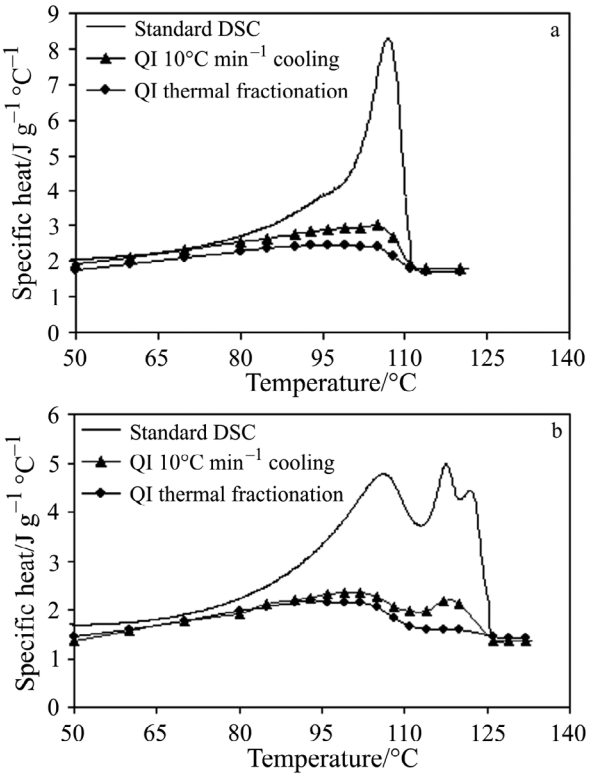

Fig. 3 Quasi-isothermal modulated specific heat curves of a – VLDPE2 and b – 50:50 LLDPE-VLDPE2 blend. Measurements were performed in the 50–135°C range in every 2–5°C step. Modulation parameters were underlying heating rate of 0°C min^{-1}, temperature amplitude of 0.5°C, period of 60 s and 20 min time. The last 10 min modulation data was used for the calculation. Thin line represents the standard DSC curve obtained at 10°C min^{-1} rate

Quasi-isothermal TMDSC experiments have recently been used to probe and to quantify processes that are truly reversible [20–22]. As previously mentioned, the C'_p curve characterises only part of the reversible events under the modulation conditions. Quasi-isothermal TMDSC specific heat capacity curves of VLDPE2 and 50:50 LLDPE-VLDPE2 blend, measured at various temperatures over the melting range after a modulation for 20 min at a constant temperature are shown in Fig. 3a and b, respectively. After removing all modulation distortions due to the irreversible effects, i.e., achieving the steady state, these curves show only a relatively smaller reversible contribution for thermally fractionated and continuously cooled samples. However, the reversible contribution of thermally fractionated samples within the melting range was a minor portion of the total curve (31% for thermally fractionated VLDPE2 and 28% for thermally fractionated 50:50 LLDPE-VLDPE2) compared to the continuously cooled samples (44% for 50:50 continuously cooled VLDPE2 and 40% for continuously cooled 50:50 LLDPE-VLDPE2). Such small amounts of reversible melting contributions have been observed before for other high molar mass polyethylenes [15, 17–23]. The approach to the steady state was checked by constructing Lissajous figures [4, 37]. The good agreement between heat capacities before and after melting suggests that melting is mostly thermodynamically reversible in these regions. A standard DSC curve (thin solid line) contains many effects including the reversible melting. Furthermore, the enthalpies of continuously cooled samples (38.8 J g^{-1} for VLDPE2 and 42.7 J g^{-1} for 50:50 LLDPE-VLDPE2) were noticeably higher than that of thermally fractionated samples (27.4 J g^{-1} for VLDPE2 and 29.3 J g^{-1} for 50:50 LLDPE-VLDPE2).

Final evaluation

The crystallisation conditions have great impact on the characteristic of crystallites. Melting of polyethylene blends and pure polymers by TMDSC provides interesting observations when the total melting endotherms are divided into their reversing and NR components. The reversing signal reflects the melting of crystals and exothermic events are completely absent in this curve. Crystallisation exotherms are only seen in the C_{pNR} curve, however, the C_{pNR} curve contains both endothermic and exothermic events. The C_{pNR} curves of fractionated blends (Fig. 2c) showed no exothermic contribution; however, large amounts of exothermic contributions were detected for blends cooled at 10°C min^{-1}. The faster cooling rates allow the branches to be included in the crystal lattice, leading to imperfect crystallites and thinner lamellae. This has also been found in an ethylene-octene copolymer having high comonomer content (7.3 mol%) by Androsch and Wunderlich and the formation of less ordered pseudo-hexagonal crystals is proposed [17]. Upon crystallisation at a slow rate there is less likelihood for the branches entering into the crystal lattice. Thus, it is reasonable to assume that the crystals formed at the slow cooling rate approach equilibrium, so that rearrangement during the scan will be minimal. As seen in the Tables 2 and 3, the relative fraction of reversing and NR components depends on the crystal type and the experimental conditions. The reversing contribution is always broader and larger

in magnitude than the total C_p for the continuously cooled samples, whereas the opposite was observed for the thermally fractionated samples. Six contributions, three reversible (thermodynamic heat capacity, heat capacity due to conformational motions, reversible melting) and three irreversible (crystal perfection, secondary crystallisation and primary crystallisation), to apparent heat capacity have been suggested by Wunderlich *et al*. [18–20]. The present study revealed the presence of some of the effects including reversible melting of polymers and blends that had been observed by quasi-isothermal TMDSC measurements. While the interpretation of TMDSC data is dependent on the experimental conditions, it provides important information that is useful in characterising polymers.

Conclusions

It was found that crystals of copolymers and their blends formed under different crystallisation conditions had different internal order, hence showed different amounts of reversing and NR contributions. The melting curves obtained for the samples cooled at 10°C min^{-1} contained possible mrr effects, which are the result of high cooling rate and slow heating rate. In contrast, the crystals formed under the very slow cooling condition approached equilibrium, so that rearrangement during the scan would be minimal. The stepwise-cooled samples, cooled at an average rate of 0.08°C min^{-1} showed no detectable rearrangement during melting. However, some true reversible contributions are observed by quasi-isothermal TMDSC measurements. Melting is generally a combination of thermodynamic and kinetic events that can be observed using TMDSC. Melting is often accompanied by recrystallisation, when the crystals are not at equilibrium. Such phenomena during a TMDSC melting scan provide valuable information on the polymer thermal history.

References

1 P. S. Gill, S. R. Sauerbrunn and M. Reading, J. Thermal Anal., 40 (1993) 931.
2 M. Reading, Trends Polym. Sci., 8 (1993) 248.
3 J. E. K. Schawe, Thermochim. Acta, 260 (1995) 1.
4 B. Wunderlich, A. Boller, I. Okazaki, K. Ishikiriyama, W. Chen, M. Pyda, J. Pak, I. Moon and R. Androsch, Thermochim. Acta, 330 (1999) 21.
5 S. L. Simon, Thermochim. Acta, 374 (2001) 55.
6 Z. Jiang, C.T. Imire and J. M. Hutchinson, Thermochim. Acta, 387 (2002) 75.
7 A. Genovese and R. A. Shanks, J. Therm. Anal. Cal., 75 (2004) 233.
8 M. Reading and R. Luyt, J. Therm. Anal. Cal., 54 (1998) 535.
9 M. C. Righetti, Thermochim. Acta, 330 (1999) 131.
10 S. Weyer, A. Hensel and C. Schick, Thermochim. Acta, 304/305 (1997) 267.
11 B. Wunderlich, Macromolecular Physics, Academic Press, New York 1980, Vol 3, p. 128.
12 B. Wunderlich, J. Polym. Sci.: Polym. Phys., 28 (2003) 383.
13 A. Toda, C. Tomita, M. Hikosaka and Y. Saruyama, Thermochim. Acta, 324 (1998) 95.
14 R. Scherrenberg, V. Mathot and A. Van Hemelrjk, Thermochim. Acta, 330 (1999) 3.

15 J. J. Janimak and G. C. Stevens, Thermochim. Acta, 332 (1999) 125.
16 G. Amarasinghe, F. Chen, A. Genovese and R. A. Shanks, J. Appl. Polym. Sci., 90 (2003) 681.
17 R. Androsch, Polymer, 40 (1999) 2805.
18 R. Androsch and B. Wunderlich, Macromolecules, 32 (1999) 7238.
19 R. Androsch and B. Wunderlich, Macromolecules, 33 (2000) 9076.
20 J. Pak and B. Wunderlich, Macromolecules, 34 (2001) 4492.
21 J. Pak and B. Wunderlich, J. Polym. Sci.: Polym. Phys., 40 (2002) 2219.
22 B. Wunderlich, I. Okazaki, K. Ishikiriyama and A. Boller, Thermochim. Acta, 324 (1998) 77.
23 B. Wunderlich, Thermochim. Acta, 396 (2003) 33.
24 B. Goderis, H. Reynaers, R. Scherrenberg and V. B. F. Mathot, Macromolecules, 34 (2001) 1779.
25 G. W. H. Hohne and L. Kurelec, Thermochim. Acta, 377 (2001) 141.
26 G. W. H. Hohne, L. Kurelec, S. Rastogi and P. J. Lemstra, Thermochim. Acta, 396 (2003) 97.
27 W. B. Hu, T. Albrecht and G. Strobl, Macromolecules, 32 (1999) 7548.
28 S. Vanden Eynde, V. B. F. Mathot, M. H. J. Koch and H. Reynaers, Polymer, 41 (2000) 4889.
29 J. Pak, M. Pyda and B. Wunderlich, Thermochim. Acta, 396 (2003) 43.
30 J. Y. Nam, S. Kadomatsu, H. Saito and T. Inoue, Polymer, 43 (2002) 2101.
31 F. Cser, M. Jollands, P. White and S. Bhattacharya, J. Therm. Anal. Cal., 75 (2002) 651.
32 K. Ishikiriyama and B. Wunderlich, Macromolecules, 30 (1997) 4126.
33 K. Ishikiriyama and B. Wunderlich, J. Polym. Sci.: Polym. Phys., 35 (1997) 1877.
34 R. A. Shanks and G. Amarasinghe, Polymer, 41 (2000) 4579.
35 K. W. Swogger, G. M. Lancaster, S. Y. Lai and T. I. Butler, J. Plastic Film and Sheeting, 11 (1995) 102.
36 J. Schellenberg and B. Wagner, J. Therm. Anal. Cal., 52 (1998) 275.
37 V. L. Hill, D. Q. M. Craig and L. C. Feely, Int. J. Pharm., 192 (1999) 21.
38 B. Wunderlich, Crystal Melting, Macromolecular Physics, Academic Press, New York, NY 1980, Vol. 3, p. 48.
39 S. Hosoda, K. Kojima and M. Furuta, Macromol. Chem., 187 (1986) 1501.
40 B. B. Sauer, W. G. Kampert, E. Neal Blanchard, S. A. Threefoot and B. S. Hsiao, Polymer, 41 (2000) 1108.
41 W. G. Kampert and B. B. Sauer, Polymer, 42 (2001) 8703.
42 M. Y. Keating, I.-H. Lee and C. S. Wong, Thermochim. Acta, 284 (1996) 47.
43 F. Chen, R. A. Shanks and G. Amarasinghe, Polymer, 42 (2001) 4579.
44 W. Liu, S. Kim, J. Lopez, B. Hsiao, M. Y. Keating, I. H. Lee, B. Landes and R. S. Stein, J. Therm. Anal. Cal., 59 (2000) 245.